



ELSEVIER

BioSystems 40 (1997) 203–210



Coding of odour intensity in a sensory neuron

Arthur Vermeulen^{a,b}, Petr Lánský^c, Henry Tuckwell^{a,d}, Jean-Pierre Rospars^{*a}

^aLaboratoire de Biométrie, Institut National de la Recherche Agronomique, 78026 Versailles Cedex, France

^bTraitement d'Images et Reconnaissance de Formes, Institut National Polytechnique, 38031 Grenoble Cedex, France

^cInstitute of Physiology and Center for Theoretical Study, Academy of Sciences, 142 20 Prague 4, Czech Republic

^dSchool of Mathematical Sciences, Institute for Advanced Studies, Australian National University, Canberra, ACT 0200, Australia

Abstract

A deterministic biophysical model of an olfactory sensory neuron under constant stimulation is presented with the aim of describing the successive conversion steps, including receptor activation, conductance change, receptor potential and firing frequency, that are involved in the coding of odorant concentration. This model is divided in two parts. The odorant-sensitive part (OSP), consisting of one cylindrical dendrite, is connected to the odorant-insensitive part (OIP), corresponding to passive dendrite, soma and axon. Each part exerts a specific effect on the coding properties of the conversion steps, i.e. their magnitude, sensitivity and dynamic range. The maximum conductance of the OSP affects positively all coding properties whereas the input resistance of the OIP, which depends on its size and shape, affects positively the sensitivity and negatively the dynamic range. These findings are helpful for understanding the input-output properties of many types of neurons.

Keywords: Sensory coding; Cable equation; Single neuron modelling; Olfaction

1. Introduction

The olfactory receptor neuron appears as a promising example for studying the input-output relationship of a neuron, because of the good experimental control of its stimulation and its simple morphology. For example, the dendrite is close to a cylinder in the case of the moth sex-pheromone receptor cell (Keil, 1984). The transduction process begins with the binding of odour

molecules to receptor proteins borne by the dendritic membrane (Fig. 1a). The activated receptor triggers a second-messenger system that ultimately opens odorant-dependent ionic channels (see Stengl et al., 1992) and a depolarization of the membrane follows, the so-called receptor potential (Kaissling, 1987). When this potential is high enough at the axon initial segment, action potentials are generated. In previous work we studied a model describing how the odorant concentration (input) is coded, under steady state conditions, in three modules — transduction, receptor potential and action potential modules

* Corresponding author.

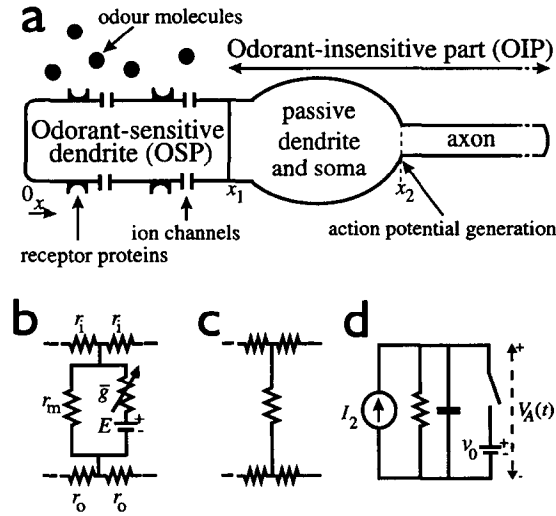


Fig. 1. Schematic representation of the model receptor neuron (a) with equivalent circuits of the cylindrical odorant-sensitive dendrite OSP (b), the odorant-insensitive part OIP (c) and the action potential generator (d). Binding of odorant molecules to receptor proteins on the OSP ultimately triggers the opening of ion channels. This conductance change \bar{g} generates a receptor potential V that spreads to the axon initial segment at x_2 on OIP where action potentials are generated. In (d), the action potential generator is driven by a dendritic current I_2 which is proportional to $V(x_2)$.

(Rospars et al., 1996). This model neuron was based on a cylindrical cable divided in two parts—the odorant-sensitive part (OSP) of finite length corresponding to the sensory dendrite and the odorant-insensitive part (OIP) of semi-infinite length corresponding to passive dendrite, soma and axon. More realistic assumptions, including an OIP of any length and shape and passive backpropagation of action potentials into the OSP, were considered in Vermeulen et al. (1996) and are further studied here. The aim of the present article is to review how the membrane conductance, receptor potential and firing frequency depend on the odorant concentration and to derive the coding properties of these responses in terms of their magnitude, sensitivity and dynamic range.

2. Model of the three conversion steps

2.1. Transduction

The first module describes the concentration-

to-conductance conversion which takes place at the OSP. The neuron is assumed to be stimulated with only one type of odorant molecules A whose concentration per unit area of membrane is $[A]$. This conversion presents two main steps, activation of receptors then conductance change. The first step is described by the classical sequence of binding and activation



where k_1 , k_{-1} , k_2 and k_{-2} denote velocity constants. The number of activated receptors at equilibrium $[AR^*]$ can be calculated (Getz and Akers, 1995; Kaissling, 1971; Rospars et al., 1996) from $[A]$, the total number of receptors $[R_T]$, and the dissociation $K_1 = k_1/k_{-1}$ and deactivation $K_2 = k_2/k_{-2}$ equilibrium constants. The curve of $[AR^*]$ vs. $[A]$ is a branch of hyperbola.

For the second step of the transduction process, it is simplest to assume that the number of opened odorant-dependent ionic channels and the corresponding conductance change g of the OSP are proportional to $[AR^*]$. The constants of proportionality depend on the mean number Γ of channels opened per activated receptor and the unit conductance γ of the channels. The curve of g as a function of $[A]$ is again a branch of hyperbola characterized by an asymptote g_M and a concentration $[A]_{g/2}$ at half-saturation $g_M/2$

$$g = \frac{g_M}{1 + \frac{[A]_{g/2}}{[A]}} \quad \text{with} \quad g_M = \frac{\gamma \Gamma [R_T]}{K_2 + 1}$$

$$\text{and} \quad [A]_{g/2} = \frac{K_1 K_2}{K_2 + 1}, \quad (2)$$

where γ and g are measured in units of the conductance at rest r_m^{-1} of the OSP (r_m is the membrane resistance per unit length).

2.2. Receptor potential

2.2.1. Neuron shape

The principal input variable is the conductance change g resulting from the concentration-to-conductance module and we want to know the resulting change of the membrane potential $V(x)$

at any point x along the neuron. All electrical parameters are assumed to be uniform so the resistances depend only on the size and shape of the neuron. We consider the situation in which the OSP is approximated by a cylinder, which is the case of the sex-pheromone receptor cell (Keil, 1984). We restrict our study to the case of a uniform conductance change $\bar{g} = g$ along the OSP, i.e. all molecules involved in transduction (A , R , second messengers, channels) are assumed to be uniformly spread along the OSP. The OIP presents a more complex shape with bulging soma and very thin axon. This complexity can be hidden in the input resistance R_{in} , which is the only characteristic of the OIP that must be known. It is defined as the ratio of the potential $V(x_1)$ at the point ($x = x_1$) where the OSP meets the OIP to the axial current $I(x_1)$ that leaves the OSP and enters the OIP (see inset, Fig. 2). R_{in} is known analytically for a dendritic tree consisting of uniform cable segments (Rall and Rinzel, 1973). In other cases R_{in} must be calculated numerically e.g. by using compartmental models (Rall, 1964; Segev et al., 1989).

2.2.2. Odorant-sensitive dendrite

For an OSP of length x_1 the steady-state re-

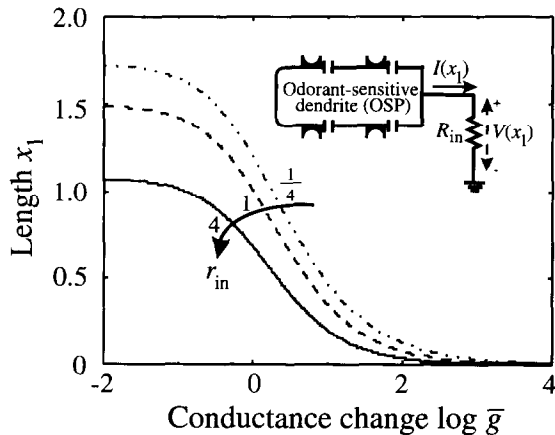


Fig. 2. Length x_1 of OSD for which the receptor potential $V(x_1)$ is 95% of its asymptotic value V_1 ($x_1 \rightarrow \infty$) as a function of conductance \bar{g} for different $r_{in} = R_{in}/(r_i + r_o)$. Further increase of x_1 has not much influence on $V(x_1)$. Inset shows that OIP is replaced by its input resistance R_{in} to calculate the receptor potential on OSP in the case of an isopotential extracellular medium.

ceptor potential $V(x)$ is the solution of the steady-state cable equation (Rall, 1989; Tuckwell, 1988)

$$V''(x) + V(x) = \bar{g}(E - V(x))$$

$$\text{for } 0 \leq x \leq x_1,$$
(3)

where x is the distance along the neuron (in space constants $\lambda = \sqrt{r_m/(r_i + r_o)}$, where r_i and r_o are the axial resistances per unit length of the internal and external media, respectively), ' indicates differentiation with respect to x and E is the reversal potential of the permeating ions. From the definitions of $R_{in} = U(x_1)/I(x_1)$ and the axial current $I(x_1) = -V'(x_1)/(r_i + r_o)$ (Tuckwell, 1988) we obtain the boundary condition $V(x_1) = -R_{in} V'(x_1)/(r_i + r_o)$. Denoting by r_{in} the dimensionless ratio $R_{in}/(r_i + r_o)$ and assuming that the distal end of the OSP ($x = 0$) is 'sealed', i.e. $V'(0) = 0$, the receptor potential V along the OSP is given by

$$V(x) = \left(1 - \frac{\cosh(\sqrt{1 + \bar{g}} x)}{D}\right) \frac{\bar{g}}{1 + \bar{g}}$$
(4)

$$\text{with } D = (r_{in} \sqrt{1 + \bar{g}}) \sinh(\sqrt{1 + \bar{g}} x_1) + \cosh(\sqrt{1 + \bar{g}} x_1)$$

for $0 \leq x \leq x_1$, (Vermeulen et al., 1996). This equation can be simplified when the length of the OSP exceeds a certain limit (which depends on \bar{g} ; Fig. 2). Then the asymptotic version of Eq. (4) for $x_1 \rightarrow \infty$ can be used as a good approximation. Denoting by V_0 the asymptotic voltage at $x = 0$, which gives approximately the potential over much of the OSP, and V_1 the asymptotic voltage at $x = x_1$, we can derive

$$V_0 = \frac{E\bar{g}}{1 + \bar{g}} \quad \text{and} \quad V_1 = V_0 \frac{r_{in} \sqrt{1 + \bar{g}}}{1 + r_{in} \sqrt{1 + \bar{g}}}.$$
(5)

V_0 is a hyperbolic function of \bar{g} ; it is the potential obtained for the point model neuron. The ratio V_1/V_M , where V_M is the limit of V_1 when $[A] \rightarrow \infty$, is shown in Fig. 3 as a function of $\log[A]$ for different r_{in} and g_M ; it tends to V_0/E

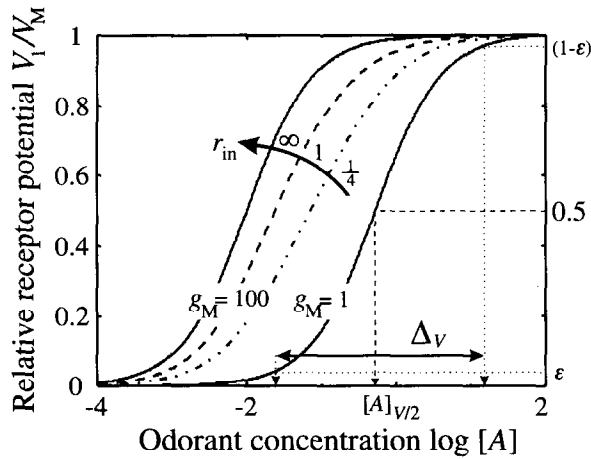


Fig. 3. Ratio V_1/V_M of asymptotic receptor potential V_1 at proximal end x_1 of OSP to its maximum value V_M ($[A] \rightarrow \infty$) as a function of odorant concentration $[A]$ for different r_{in} and g_M . Sensitivity measured by concentration $[A]_{V/2}$ at half-maximum response and dynamic range Δ_V measured by distance in log units between $[A]$ at threshold ($V_1/V_M = \epsilon$) and at saturation ($V_1/V_M = 1 - \epsilon$), are indicated for $g_M = 1$. Smaller r_{in} induces a wider dynamic range for large g_M . These differences disappear for small g_M (curves shown are superimposed for $g_M = 1$).

when $r_{in} \rightarrow \infty$ and its slope is less steep than that of V_0/E for large values of g_M . Decreasing g_M , this difference disappears and the response curve shifts towards higher concentrations.

2.2.3. Odorant-insensitive part

The OIP contains no current source (Fig. 1c) so the receptor potential along this part is proportional to $V(x_1)$

$$V(x) = C(x) V(x_1) \quad \text{for } x > x_1, \quad (6)$$

where the proportionality function $C(x)$ depends on the shape of the OIP. Function $C(x)$ gives the voltage attenuation (Rall and Rinzel, 1973) between x_1 and x and can be calculated for instance by describing the neuron as a linear two-port electrical network (Carnevale and Johnston, 1982; Koch et al., 1982). If the OIP is a cylindrical semi-infinite cable (Rospars et al., 1996), we find $C(x) = \exp(-(x - x_1))$. An important consequence of Eq. (6) is that the sensitivity and dynamic range of V are the same at x_1 and all points along the OIP.

2.3. Action potentials

The action potential generator, which is assumed to be located at the axon initial segment (at $x = x_2$ in Fig. 1a), can be described by the classical leaky integrator (Tuckwell, 1988). This is a RC circuit with a switch in parallel, driven by the dendritic current I_2 at x_2 (see inset, Fig. 1d), which gives only an estimate of the time of firing, not the shape of the spike. When the potential at the initial segment $V_A(t)$ exceeds the firing threshold S_2 the switch closes and $V_A(t)$ is instantly brought to the resting level v_0 . A quasi steady-state is assumed so that the switch opens again and the potential $V_A(t)$ is driven by the input current from the OSP which is determined by Eq. (6). The firing frequency f is given by

$$f = \left\{ \ln \left(\frac{V(x_2) - v_0}{V(x_2) - S_2} \right) \right\}^{-1} \\ \approx \frac{V(x_2)}{S_2 - v_0} - \frac{1}{2} \quad \text{for } V(x_2) \gg S_2. \quad (7)$$

It increases very quickly at first then depends linearly on the receptor potential. The linear approximation in Eq. (7) differs from f by less than 5% for $V(x_2) > 2 S_2$ (Rospars et al., 1996). The concentration-to-frequency conversion curve is not sigmoid in log scale, which is different from the experimentally observed curves (see discussion in Section 4).

One of the main simplifications of this model, which facilitates the finding of an analytical expression for f as a function of $V(x_2)$, is to assume that $V(x_2)$ is not affected by the time variation of the potential at the initial segment, i.e. the initial segment is not incorporated in the cable but is an isolated circuit driven by the dendritic current. In reality action potentials propagate passively backward into the dendrite. To study the influence of backpropagation on firing frequency a phenomenological model of the initial segment, simulating the action potential as a square pulse, was incorporated in the cable and the firing frequency

was computed numerically (Vermeulen et al., 1996). It was found that the firing frequency with backpropagation is increased with respect to that without backpropagation given by Eq. (7). However, the ratio f/f_M , where f_M denotes the asymptotic frequency for $[A] \rightarrow \infty$, is approximately the same in both cases. Exceptions were found with a few parameter sets for which the dynamic range is very narrow, i.e. the neuron either does not respond at all or responds with maximal firing frequency.

3. Coding properties of the model

The model of an olfactory neuron studied describes quantitatively the three main physiological responses, conductance g at the OSP, potential V along the neuron and firing frequency f at the axon, as a function of the odorant concentration. These responses can be characterized by three coding properties, their magnitude, sensitivity and dynamic range. The model shows that each conversion step plays a specific role in the neuron overall concentration-to-frequency conversion.

3.1. Magnitude

The magnitudes of the responses depend on many factors that appear explicitly in Eqs. (2), (5), (6) and (7), and the observation that the dendritic backpropagation of spikes increases f . The responses g , V and f being expressed in different units cannot be easily compared. However, an explicit factor of amplification appears in Eq. (2) that describes via g_M the magnitude of the conductance response and shows how the concentration-to-conductance conversion transforms the weak signal of the odorant-receptor interaction into the stronger signal carried by the permeating ions. According to Eq. (2) this amplification depends on constants K_2 , Γ (channels per receptor) and γ (channel conductance). This description suggests that the gain in magnitude results mainly from the transduction module and specifically from the maximum conductance g_M of the OSP.

The magnitude of V given by Eq. (4) is independent of the length x_1 of the OSP for x_1

sufficiently long; for example, with $r_{in} = 1$ and $\bar{g} = 20$, $V(x_1)$ exceeds 95% of its maximum value for $x_1 > 0.3$. In the moth *Antheraea* the space constant λ is about 300 μm with a membrane resistance r_m of 3 $\text{k}\Omega\text{cm}^2$ (Kaissling, 1987); a higher r_m , such as 100 $\text{k}\Omega\text{cm}^2$ as proposed for the salamander *Ambystoma* (Firestein and Werblin, 1987), would result in a still smaller dendritic length. Thus, the length of the OSP (300 μm in *Antheraea*, 50–200 μm in *Ambystoma*) may be interpreted in a purely electrical model as an adaptation to small intensities of stimulation, i.e. small \bar{g} .

3.2. Sensitivity

Sensitivity, as understood here, specifies the position of the concentration-response curves along the concentration axis and can be measured by the odorant concentrations at threshold, at half-maximum response and at saturation. The model shows that three parameters control the sensitivity of the response curves. First, the conductance curve is shifted towards low concentrations when the constant K_1 is increased (it is independent of K_2 , Rospars et al., 1996). Second, the receptor-potential curve is always shifted to the left of the conductance curve and the shift increases with the maximum conductance g_M of the OSP, so that g_M plays a major role in the sensitivity of the neuron (Figs. 3 and 4a). Third, the concentrations at half-maximum response $[A]_{V/2}$ (Fig. 3) and at saturation (but not at threshold) of the receptor potential are slightly shifted to the left when the input resistance of the OIP increases (see Fig. 4c for $[A]_{V/2}$), which occurs for example when the spatial extent of the neuron decreases. Conversely, the voltage-to-frequency conversion corresponds to a slight loss in sensitivity (Rospars et al., 1996) which does not depend on spike backpropagation (Vermeulen et al., 1996). This loss appears as the price to pay for converting a local signal into a non-decremental long-range signal. However, much of the gain in sensitivity due to the conductance-to-voltage conversion is conserved, so that globally the conductance-to-frequency corresponds to a gain in sensitivity. In conclusion, the input-output conversion

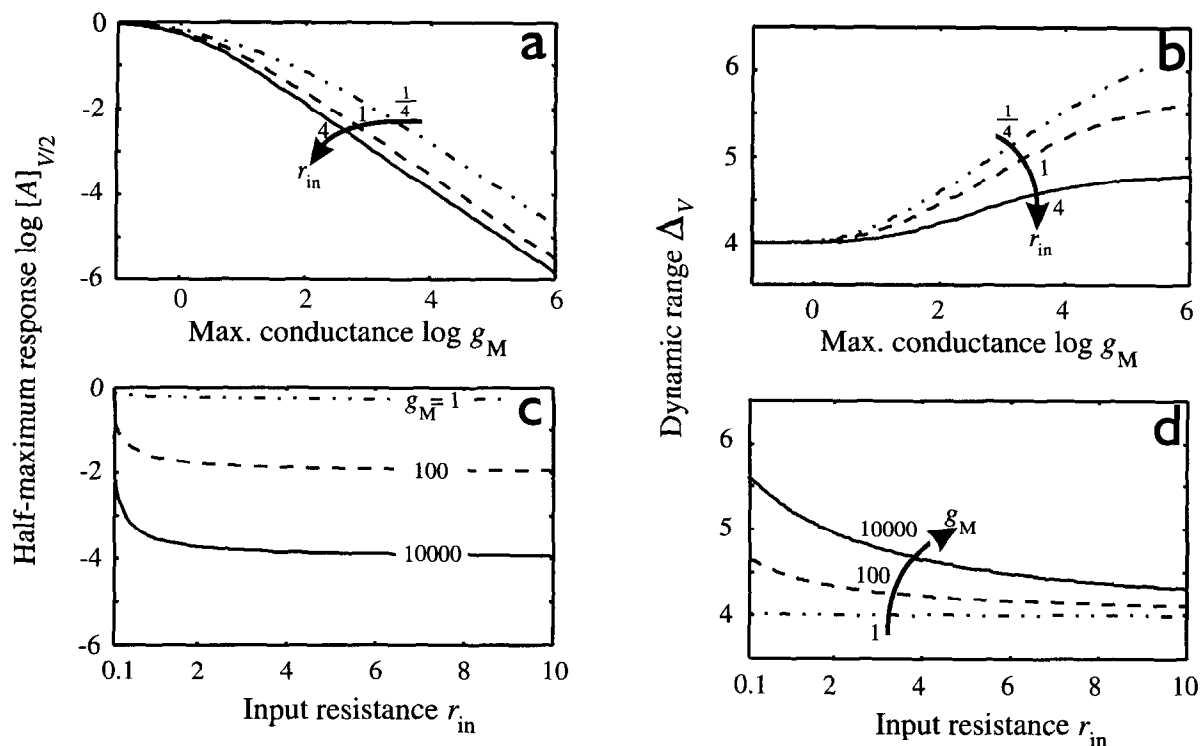


Fig. 4. Coding properties of receptor potential V_1 as a function of maximum conductance change g_M of OSP and input resistance r_{in} of OIP. (a,b) Sensitivity measured by concentration $[A]_{V/2}$ at half-maximum response. (c,d) Dynamic range Δ_V . Sensitivity is mainly controlled by g_M but the dynamic range varies with r_{in} and g_M . For firing frequency the curves are qualitatively similar except that $[A]_{f/2} > [A]_{V/2}$ and $\Delta_f < \Delta_V$. Parameters: $\epsilon = 0.01$.

of the model neuron is characterized by an overall gain in sensitivity that results mainly from the conductance-to-voltage conversion. So, the maximum conductance g_M appears to control both the overall gain in sensitivity and in magnitude.

3.3. Dynamic range

The dynamic (or coding) range is measured in log units by the ratio of the concentrations at saturation and at threshold. We define the threshold level as the concentration for which the relative response (e.g. V/V_M) is equal to a value ϵ close to zero and the saturation level as the concentration for which it is $1 - \epsilon$, close to 1 (Fig. 3). With $\epsilon = 11\%$ the dynamic range of the conductance response Δ_g is exactly 4 log units and is independent of K_1 and K_2 (Rosparis et al.,

1996). As shown in Fig. 4b, the dynamic range Δ_V of the receptor potential along the OIP increases with g_M . Δ_V depends also on the input resistance r_{in} and is maximum for $r_{in} \ll 1$ (Fig. 4d). Finally, a wide coding range Δ_f of the firing frequency is obtained with a large g_M and a small r_{in} . Because the f vs. $[A]$ curve is truncated to the left, the threshold level for f lags behind that for V , whereas their saturation levels are almost the same. So, Δ_f increases with g_M up to $g_M \approx 10^6$. For a semi-infinite OIP ($r_{in} = 1$) Δ_f cannot exceed 5.7 log units (for $g_M \rightarrow \infty$ and $S_2 \rightarrow 0$; Rosparis et al., 1996). However, in actual receptor neurons r_{in} is smaller than 1. With $r_{in} = 0.33$ (from data in Kaissling, 1987), Δ_f cannot exceed 6.3. This is close to the 6 or more log units experimentally measured in the moth sex-pheromone receptor (Kaissling, 1987).

4. Discussion

The model presented calls for several improvements. These belong to two categories:

4.1. Deterministic improvements

These include more detailed descriptions of the transduction cascade, dendritic morphology, action potential generation and neuron environment. In the present work, the neuron was assumed to be isolated from the auxiliary cells that surround it. In particular, the voltage source might not be on the OSP, as in the present model, but located on the OIP and the auxiliary cells as discussed, for instance, by Kaissling (1971), Kaissling and Thorson (1980) and Thurm and Küppers (1980). A comparison with the present model will be made elsewhere.

4.2. Stochastic improvements

The deterministic model presented assumes that the numbers of odorant molecules, activated receptor proteins and elementary receptor potentials are large enough, so that the system is at equilibrium and all curves can be considered as continuous. For these reasons a deterministic model, however sophisticated, is only an approximation at very low odour concentration. When describing the effect of individual odorant molecules, receptors and channels (Kaissling, 1971; Menini et al., 1995) stochastic models must be used (Lánský and Rospars, 1993, 1995a, 1995b; Rospars and Lánský, 1993). In these stochastic generalizations the neuron starts firing below the deterministic threshold level (Tuckwell and Richter, 1978; Gerstner and Van Hemmen, 1992; Segundo et al., 1994; Wiessenfeld and Moss, 1995; Lánský and Rospars, 1995a) because the random fluctuations of the receptor potential V can trigger spikes even when its mean value is below the firing threshold. It follows that the firing frequency increases smoothly as a function of concentration as observed experimentally (sigmoid shape). The curves of V and f vs. $[A]$ become very similar which contributes to diminish the differences between their coding properties.

References

- Carnevale, N.T. and Johnston, D., 1982, Electrophysiological characterization of remote chemical synapses. *J. Neurophysiol.* 47, 606–621.
- Firestein, S. and Werblin, F.S., 1987, Gated currents in isolated olfactory receptor neurons of the larval tiger salamander. *Proc. Natl. Acad. Sci. USA* 84, 6292–6296.
- Gerstner, W. and Van Hemmen, J.L., 1992, Universality in neural networks: The importance of the ‘mean firing rate’. *Biol. Cybern.* 67, 195–205.
- Getz, W.M. and Akers, R.P., 1995, Partitioning non-linearities in the response of honey bee olfactory receptor neurons to binary odors. *BioSystems* 34, 27–40.
- Kaissling, K.-E., 1971, Insect olfaction, in: *Handbook of Sensory Physiology, Vol. IV, Chemical Senses, Part. 1, Olfaction*, L.M. Beidler (ed.) (Springer-Verlag, Berlin), pp. 351–431.
- Kaissling, K.-E., 1987, R.H. Wright lectures on insect olfaction, K. Colbow (ed.) (Simon Fraser University, Burnaby).
- Kaissling, K.-E. and Thorson, J., 1980, Insect olfactory sensilla: Structural, chemical and electrical aspects of the functional organization, in: *Receptors for neurotransmitters, hormones and pheromones in insects*, D.B. Sattelle, L.M. Hall, and J.G. Hildebrand (eds.) (Elsevier/North-Holland, Amsterdam), pp. 261–282.
- Keil, T.A., 1984, Reconstruction and morphometry of silkmouth olfactory hairs: A comparative study of sensilla trichodea on the antennae of male *Antheraea polyphemus* and *Antheraea pernyi* (Insecta, Lepidoptera). *Zoomorphology* 104, 147–156.
- Koch, C., Poggio, T. and Torre, V., 1982, Retinal ganglion cells: A functional interpretation of dendritic morphology. *Phil. Trans. R. Soc. London B* 298, 227–264.
- Lánský, P. and Rospars, J.-P., 1993, Coding of odor intensity. *BioSystems* 31, 15–38.
- Lánský, P. and Rospars, J.-P., 1995a, Ornstein-Uhlenbeck model neuron revisited. *Biol. Cybern.* 72, 397–406.
- Lánský, P. and Rospars, J.-P., 1995b, Mathematical approach to transduction processes in olfactory receptor neurons. *J. Jap. Soc. Instr. Control Eng.* 34, 800–804.
- Menini, A., Picco, C. and Firestein, S., 1995, Quantal-like current fluctuations induced by odorants in olfactory receptor cells. *Nature* 373, 435–437.
- Rall, W., 1964, Theoretical significance of dendritic trees for neuronal input-output relations, in *Neural theory and modeling*, R. Reiss (ed.) (Stanford Univ. Press, Stanford).
- Rall, W., 1989, Cable theory for dendritic neurons, in *Methods in neural modeling: From synapses to networks*, C. Koch, I. Segev (eds.) (The MIT Press, Cambridge), pp. 9–62.
- Rall, W. and Rinzel, J., 1973, Branch input resistance and steady attenuation for input to one branch of a dendritic neuron model. *Biophys. J.* 13, 648–688.
- Rospars, J.-P. and Lánský, P., 1993, Stochastic model neuron without resetting of dendritic potential: application to the olfactory system. *Biol. Cybern.* 69, 283–294.

- Rospars, J.-P., Lánský, P., Tuckwell, H.C. and Vermeulen, A., 1996, Coding of odor intensity in a steady-state deterministic model of an olfactory receptor neuron, *J. Comput. Neurosci.* 3, 51–72.
- Segev, I., Fleshman, J.W. and Burke, R.E., 1989, Compartmental models of complex neurons, in: *Methods in neuronal modelling; From synapses to networks*. C. Koch and I. Segev (eds.) (The MIT Press, Cambridge), pp. 63–96.
- Segundo, J.P., Vibert, J.-F., Pakdaman, K., Stiber, M. and Diez Martínez, O., 1994, Noise and the neurosciences: a long history, a recent revival and some theory, in: *Origins: brain and self-organization*, K. Pribram (ed.) (Lawrence Erlbaum, Hillsdale), pp. 300–331.
- Stengl, M., Hatt, H. and Breer, H., 1992, Peripheral processes in insect olfaction. *Annu. Rev. Physiol.* 54, 665–681.
- Thurm, U. and Küppers, J., 1980, Epithelial physiology of insect sensilla, in: *Insect Biology in the Future*, M. Locke and D. Smith (eds.) (Academic Press, New York), pp. 735–764.
- Tuckwell, H.C., 1988. *Introduction to theoretical neurobiology* (Cambridge University Press, Cambridge).
- Tuckwell, H.C. and Richter, W., 1988. Neuronal interspike time distributions and the estimation of neurophysiological and neuroanatomical parameters. *J. Theor. Biol.* 71, 167–183.
- Vermeulen, A., Rospars, J.-P., Lánský, P. and Tuckwell, H.C., 1996, Coding of stimulus intensity in an olfactory receptor neuron: role of neuron spatial extension and dendritic backpropagation of action potentials. *Bull. Math. Biol.* 58, 493–512.
- Wiessenfeld, K. and Moss, F., 1995, Stochastic resonance and the benefits of noise: from ice ages to crayfish and SQUIDS. *Nature* 373, 33–36.